Open Access Library Journal
2024, Volume 11, e11807
ISSN Online: 2333-9721
ISSN Print: 2333-9705

Model-Derived Characterization of Particulate Matter ($PM_{2.5}$) and Its Species over Kenya during 1980-2020

Faith A. Abok[1*], John W. Makokha[1], Richard Boiyo[2,3]

[1]Department of Science, Technology and Engineering, Kibabii University, Bungoma, Kenya
[2]Department of Physical Sciences, Meru University, Meru, Kenya
[3]Department of Environment, Energy, Natural Resources and Climate Change, County Government of Vihiga, Vihiga, Kenya
Email: *boiyor@yahoo.com

How to cite this paper: Abok, F.A., Makokha, J.W. and Boiyo, R. (2024) Model-Derived Characterization of Particulate Matter ($PM_{2.5}$) and Its Species over Kenya during 1980-2020. *Open Access Library Journal*, **11**: e11807.
https://doi.org/10.4236/oalib.1111807

Received: June 8, 2024
Accepted: July 27, 2024
Published: July 30, 2024

Abstract

Increasing airborne particulate matter (PM) concentration in Kenya is an unfortunate consequence of rapid urbanization, coupled with a lack of strict implementation of air quality regulations. This has led to detrimental effects on human health, environment and local climate. To gain an in-depth understanding of these effects, there is a need for a detailed characterization of PM in terms of abundance, sources, and properties, especially over the less characterized areas such as The Republic of Kenya (Kenya). This study presents long-term (1980-2020) spatial-temporal distributions and trends of $PM_{2.5}$ over Kenya retrieved from the MERRA-2 model. The spatial patterns of annual mean $PM_{2.5}$ loading were generally characterized by low (<7 $\mu g \cdot m^{-3}$), moderate (7 - 9 $\mu g \cdot m^{-3}$), and high (>11 $\mu g \cdot m^{-3}$) $PM_{2.5}$ concentrations indicating distinct features of $PM_{2.5}$ load. High (>11 $\mu g \cdot m^{-3}$) $PM_{2.5}$ concentrations were observed over the arid and semi-arid areas of the Northwest part of the country dominated by dust. Whereas, low (<7 $\mu g \cdot m^{-3}$) PM concentrations were observed over the Central and South Western parts of the country, with high vegetation and relatively high altitudes and precipitation. The seasonal mean $PM_{2.5}$ over Kenya was found to be high (low) during the local dry (wet) seasons with mean values of >12 $\mu g \cdot m^{-3}$ and <6 $\mu g \cdot m^{-3}$, respectively. The magnitude of inter-annual variability in PM and its components over Kenya was found to be influenced by changes in emissions and local meteorology. The major $PM_{2.5}$ emissions components were natural dust emissions over the arid and semi-arid areas in Northern Kenya with low annual precipitation. Linear trend analysis revealed an increase in $PM_{2.5}$ over the years. Furthermore, the annual spatial trends revealed a general increase in $PM_{2.5}$ over Kenya, being positive and significant over the dust-dominated areas of Northern Kenya. Later the spatial correlation between $PM_{2.5}$ and its compo-

nents revealed areas of similarities/dissimilarities and the magnitude of a correlation coefficient. $PM_{2.5}$ correlated positively with dust in most parts of the country, followed by Sulphate (SO_4), showing the significant contribution of the two components to $PM_{2.5}$. On the other hand, a low (<2.5) correlation was observed between $PM_{2.5}$ and Black Carbon (BC) and Organic Carbon (OC). Further analysis of annual and seasonal spatial variation, linear trends, and correlation of $PM_{2.5}$ and components revealed dust as the major component of $PM_{2.5}$ concentrations over the study domain. The study has improved the understanding of $PM_{2.5}$ concentrations over the domain. It could provide significant information suitable for policy-making on air quality regulations in Kenya, especially on dust reduction mechanisms over the dominant areas.

Subject Areas

Atmospheric Science

Keywords

Kenya, Trends, MERRA-2, $PM_{2.5}$ MERRA-2

1. Introduction

Airborne particulate matter (PM) is one of the main pollutants responsible for ambient air quality, especially in urban areas where a significant percentage of the world's population lives [1]. Although PM can be classified in several ways, the classification based on aerodynamic diameter is one of the main criteria to describe its parameter. The Environmental Protection Agency (EPA) has been discriminating particles mainly into PM_1, $PM_{2.5}$, and PM_{10} referring to PM with aerodynamic diameter ≤ 1, 2.5, and 10 μm, respectively. [2]

The PM_1, also referred to as sub-micron or ultra-fine particles, originates from a variety of sources including chemical processes and numerous anthropogenic combustion sources such as vehicles, power plants, industries, residential cooking/heating activities, and biomass burning [3]. They are more harmful since they remain in the atmosphere for longer periods (residence time of one week) and reach deeper into the respiratory system carrying with them more toxins from anthropogenic emissions [4] [5]. On the other hand, $PM_{2.5}$ is a complex mixture of chemical species originating from distinct primary emission sources such as fuel combustion in vehicles and industrial emissions [2]. Likewise, they also emanate from secondary processes such as photochemical reactions in the atmosphere [6]. $PM_{2.5}$ penetrates deep into the respiratory organs causing respiratory and cardiovascular diseases such as pulmonary fibrosis, asthma, chronic obstructive, type 2 diabetes and cancer [7] [8]. Over the years, they have been known to cause premature deaths [9] [10] and are one of the major agents for climate perturbations [11] [12]. PM_{10} are coarse-mode particles originating mainly from natural sources such as sea salt and dust from unsealed roads and construction activities [2]. Elevated levels of PM_{10} particles in the atmosphere

can irritate the eyes and throat, as well as raise health effects associated with respiratory diseases [2].

Significant cases of these episodes are reported in low and middle-income countries (LMICs) where effective monitoring and mitigation strategies are not fully functional. In these countries, the levels of PM concentration are known to exceed the World Health Organization (WHO) upper limits of 10 and 20 $\mu g \cdot m^{-3}$ for $PM_{2.5}$ and PM_{10}, respectively [1]. This creates the need to routinely monitor PM, especially over Sub-Saharan Africa (SSA) and other LMICs with elevated concentrations and to come up with scientifically sustainable remedial measures.

Several studies focusing on the level of PM concentration have been reported in different parts of the globe. Studies by Gupta *et al.* [13] showed a good correlation between satellite data and ground-based values, which demonstrated that satellite data can be used for monitoring air quality. Wang *et al.* [14] reported a higher concentration of $PM_{2.5}$, which accounts for much of China's poor air quality and the spatiotemporal characteristics of urban $PM_{2.5}$ concentrations, has constituted a matter of significant interest within the Chinese research and policy communities. On the other hand, He *et al.* [15] derived $PM_{2.5}$ from MERRA-2 to establish the impact of meteorological variables on $PM_{2.5}$ and its major components based on a multiple linear regression (MLR) model. They observed an increasing trend of $PM_{2.5}$ and its components for the entire study period of 38 years in China.

Limited studies have been conducted in Africa on PM pollutants due to limited air quality monitoring stations and lack of air quality standards regulations [16]. An overview of air pollution in most African countries reveals that air pollution levels often exceed international guidelines. The pollution levels may be rising because of increased motor vehicle traffic, biomass burning, industrial activities and desertification; with associated health and environmental effects. [10]

Onyango *et al.* [17] conducted two-year PM measurements at three sites in the Republic of Uganda representing wide dynamics of urbanization. They reported an annual averaged PM levels were found higher than the WHO air quality guidelines. It was observed that the concentrations were higher during dry seasons. On the other hand, Singh *et al.* [18] carried out an air quality assessment in three capital cities of East Africa (EA) countries *i.e.*, Kenya (Nairobi), Uganda (Kampala), and the Republic of Tanzania (Dodoma). The measured data revealed that the mass concentrations of $PM_{2.5}$ and PM_{10} in all the cities were reported high and hazardous to human health. A recent report by Tesema *et al.* [19] reveals that EA shares a considerable burden of childhood mortality, accounting for more than half of all under-five children mortality in SSA region. Air pollution has been considered a major public health concern as a top risk factor for mortality in these countries and accounts for almost one million deaths annually [9]. Despite the health risks, air quality programs, particularly in SSA, have to be implemented for systematic PM data collection to reduce the air pollution burden.

The Republic of Kenya, hereafter simply Kenya, is one of the countries in the

SSA region, and more specifically in EA, that deserves better characterization of PM in terms of spatiotemporal distribution, trends, and associated effects. It is currently experiencing an unprecedented increase in PM concentration attributed to increased urbanization, industrialization, population, and desertification [10]. Despite this, the country lags behind the rest of the world in air quality research resulting in unquantified effects on human health, the environment and local climate [20] [21]. Previous studies [7] [21] [22] have documented elevated concentrations of $PM_{2.5}$ and PM_{10} over the country, exceeding the WHO standards [1]. The studies mentioned above were pilot studies based on data collected for a very short period. In addition, these studies were mainly based in Nairobi, with most cities in Kenya being ignored, despite the possibility of high inter-city PM disparity, emanating from distinct emission sources, and prevailing climatic conditions. Furthermore, the instrumentation used was expensive and sophisticated, and required technical workforce for monitoring. Such high-cost studies compound and aggravate the difficulty of LMICs such as Kenya to effectively monitor air pollutants continuously in many areas. The use of alternative sources of data such as satellites and model data provides an alternative opportunity to monitor PM at multiple sites with high precision, and low cost for impact assessment and policy making.

The objectives of the present study are to characterize $PM_{2.5}$ mass concentration over Kenya using long-term (1980-2020) data retrieved from the MERRA-2 model. Specifically, the study assesses the spatiotemporal distributions and trends in $PM_{2.5}$, as well as the correlation between $PM_{2.5}$ and its components (Dust, sea salt, organic carbon, black-carbon and sulphate). The study further examines the contribution of PM components to the overall $PM_{2.5}$ concentrations. This is essential for policymaking, especially in highly vulnerable urbanized environments dominated by anthropogenic activities. The rest of the paper is organized as follows: Section 2 gives a description of the study domain and the prevailing meteorological conditions, data, and methodology. Section 3 details the results and discussion of the study, whereas Section 4 summarizes the main findings drawn from the present work.

2. Study Area, Data and Methods

2.1. Study Area

The study covered the country Kenya, with the entire domain at azimuth 34˚E - 42˚E and latitude 5˚S - 5˚N. The domain is neighbored by Tanzania to the south, Uganda to the west, Somalia to the east, and Ethiopia to the north. The country is the second most populous among the countries in East Africa (EA), with a population totaling 47.6 million [23].

The main sources of PM in the study domain emanate from anthropogenic activities such as industrial-vehicular emissions, biomass burning, and suspended dust [7] [24]. The climate of the area is predominantly tropical, characterized by moderate temperatures throughout the year. However, low temperatures are recorded in the months from June to September (JJAS), whereas the

highest temperatures are noticed in January and February (JF) represented as the dry season [25] [26]. Rainfall is mainly found in bimodal distribution, experienced from March to May (MAM) locally referred to as "long rains" and October to December (OND), referred to as "short rains" [25] [27]. Based on the prevailing meteorological conditions, a year has been divided into four seasons: January-February (JF) and June-July-August-September (JJAS) represented as the local dry seasons, characterized by reduced rainfall and enhanced $PM_{2.5}$ concentrations. On the other hand, March-April-May (MAM) and October-November-December (OND) represent the local wet seasons, characterized by enhanced rainfall and reduced $PM_{2.5}$ concentrations [26] [28].

2.2. Data and Methods

MERRA-2

The Modern-Era Retrospective Analysis and Research and Application, version 2 (MERRA-2) atmospheric reanalysis product was newly released by the National Aeronautics and Space (NASA) Global Modeling and Assimilation Office (GMAO) in 2017. Based on the NASA GMAO Earth system model version 5 (GEOS 5) and the Goddard Chemistry, Aerosol, Radiation and Transport (GOCART) aerosol module, the gridded aerosol data of MERRA-2 were assimilated with satellite and ground observations. More details on the MERRA-2 $PM_{2.5}$ can be found in several works including [29] and references therein.

The MERRA-2 $PM_{2.5}$ concentrations were calculated using the equation below;

$$PM_{2.5} = 1.375 \times SO_4 + 1.6 \times OC + BC + Dust_{2.5} + SS_{2.5} \quad (1)$$

where SO_4, OC, BC, $Dust_{2.5}$, and $SS_{2.5}$ represent sulfate, organic carbon, black carbon, dust, and sea-salt particulate matter with a diameter of less than 2.5 μm from the GOCART aerosol module, respectively. Notably, the nitrate PM primarily emitted by vehicle exhaust and industrial production is lacking in the MERRA-2 $PM_{2.5}$ reanalysis. The selected pm components satellite data was retrieved from GIOVANNI (Goddard Earth Sciences Data and Information Service Centre, or GES DISC), directly on the web portal https://earthdata.nasa.gov/.

2.3. Methodology

Several statistical metrics were used to quantify the accuracy of model-derived PM. They included correlation analysis, root-mean-square error (RMSE), mean absolute error (MAE), relative mean bias (RMB), and linear regression analysis. The correlation analysis is a statistical tool that studies the relationship between two variables. Two variables are said to be correlated if the change in one variable results in a change in the other variable. Correlation analysis is defined by a correlation coefficient ranging from −1 to +1. When the value of r is +1 or −1, it indicates a perfect positive or negative correlation between given pairs of variables, respectively, with higher suggesting better agreement. The correlation coefficients between two variables (e.g, X and Y) are calculated as:

$$\mathrm{corr}(X,Y)=\frac{\mathrm{cov}(X,Y)}{\sigma_x,\sigma_y} \tag{2}$$

where represents the covariance between X and Y, and are standard deviations of X and Y, respectively. In this work, correlation analysis was aimed at establishing the relationship between PM and its components.

Linear regression analysis was adopted to estimate trends, where;

$$Y_t = c + \omega * X_t + \varepsilon \tag{3}$$

with Y_t being the dependent variable, c is the offset (y-intercept) which represents the value Y_t at the beginning of the time series. X_t is the independent variable representing time, ωis the trend estimate of the geophysical variable, whereas ε is the noise in the time series. Trends are considered significant at p-value of 0.005 or a 95% confidence interval when $|\omega/\delta| > 2$, whereas trends are considered significant at a 90% confidence level when $1.5 < |\omega/\delta| < 2$, where δ is the standard deviation of the slope "ω" obtained from the linear regression. This linear regression analysis has the practical advantage of assessing the direction and magnitude of variations in long-term data [28] [30]-[33] and therefore considered suitable for executing pixel-wise analysis.

The Root Mean Square Error (RMSE) and mean absolute error (MAE) between the model and observed PM were also computed. The RMSE gives the mean differences between the model output and the observed values, regardless of the sign of the differences. The RMSE and MAE used in the present study are defined by equations below

$$\mathrm{RMS}=\sqrt{\frac{\sum_{i=1}^{n}\left(\mathrm{PM}_{x\,\mathrm{model}}-\mathrm{PM}_{x\,\mathrm{observed}}\right)^2}{n}} \tag{4}$$

$$\mathrm{MAE}=\frac{1}{n}\sum_{i=1}^{n}\left|\mathrm{PM}_{x(\mathrm{model})i}-\mathrm{PM}_{x(\mathrm{observed})i}\right| \tag{5}$$

where n is the number of observations and PM_X (X = 2.5).

3. Results and Discussion

3.1. Spatiotemporal Changes in $PM_{2.5}$ and Its Components

3.1.1. Annual Patterns

Figure 1 illustrates the annual distribution of MERRA $PM_{2.5}$ and its components during the study period from 1980 to 2020. The MERRA $PM_{2.5}$ and its components exhibited different spatial variability, attributed to differences in anthropogenic activities.

The spatial patterns of annual mean $PM_{2.5}$ mass concentration were generally characterized by low, moderate and high concentration indicating distinct features of $PM_{2.5}$ over the study region. Low (<7 μg·m^{-3}) $PM_{2.5}$ concentrations were observed over the highly vegetated parts of the Central and the Southwest parts of Kenya geographically situated at relatively higher altitudes [34] and relatively more precipitation. Moderate (7 - 9 μg·m^{-3}) values of $PM_{2.5}$ were experienced in the Western, the Eastern, and the North Rift parts of the study domain; charac-

terized by moderate temperatures. On the other hand, moderate to high (9 - 11 $\mu g \cdot m^{-3}$) were also observed in the Southeast region and around the Northern part of the country. High $PM_{2.5}$ concentrations (>11 $\mu g \cdot m^{-3}$) were observed over arid and semi-arid areas of the Northwest part of the country with high temperatures. This could be attributed to long-range transport of dust together with those locally produced [35]. The concentration increases much higher (>17 $\mu g \cdot m^{-3}$) around the Lake Turkana region. The carbonaceous $PM_{2.5}$ from the alkaline Lake Turkana resulted in the advection of high $PM_{2.5}$ concentrations [34] as demonstrated by **Figure 1(a)** and **Figure 1(e)**. Dust concentration **Figure 1(e)** is also high (>12 $\mu g \cdot m^{-3}$) around the Lake Turkana region. To this fact, it was necessary to clarify the composition of $PM_{2.5}$. Dust $PM_{2.5}$ occupied approximately 46.71% of $PM_{2.5}$ concentration and its high values were observed around the Lake Turkana region. This suggests that $dust_{2.5}$ is the major component of $PM_{2.5}$ in Kenya. Moderate to high concentrations of dust (6 - 8 $\mu g \cdot m^{-3}$) are observed in the Northern part of the country due to high temperatures prevailing in those regions. The rest of the regions within the country which are around the equator and Southern hemisphere were observed with low (<6 $\mu g \cdot m^{-3}$) $dust_{2.5}$ concentration.

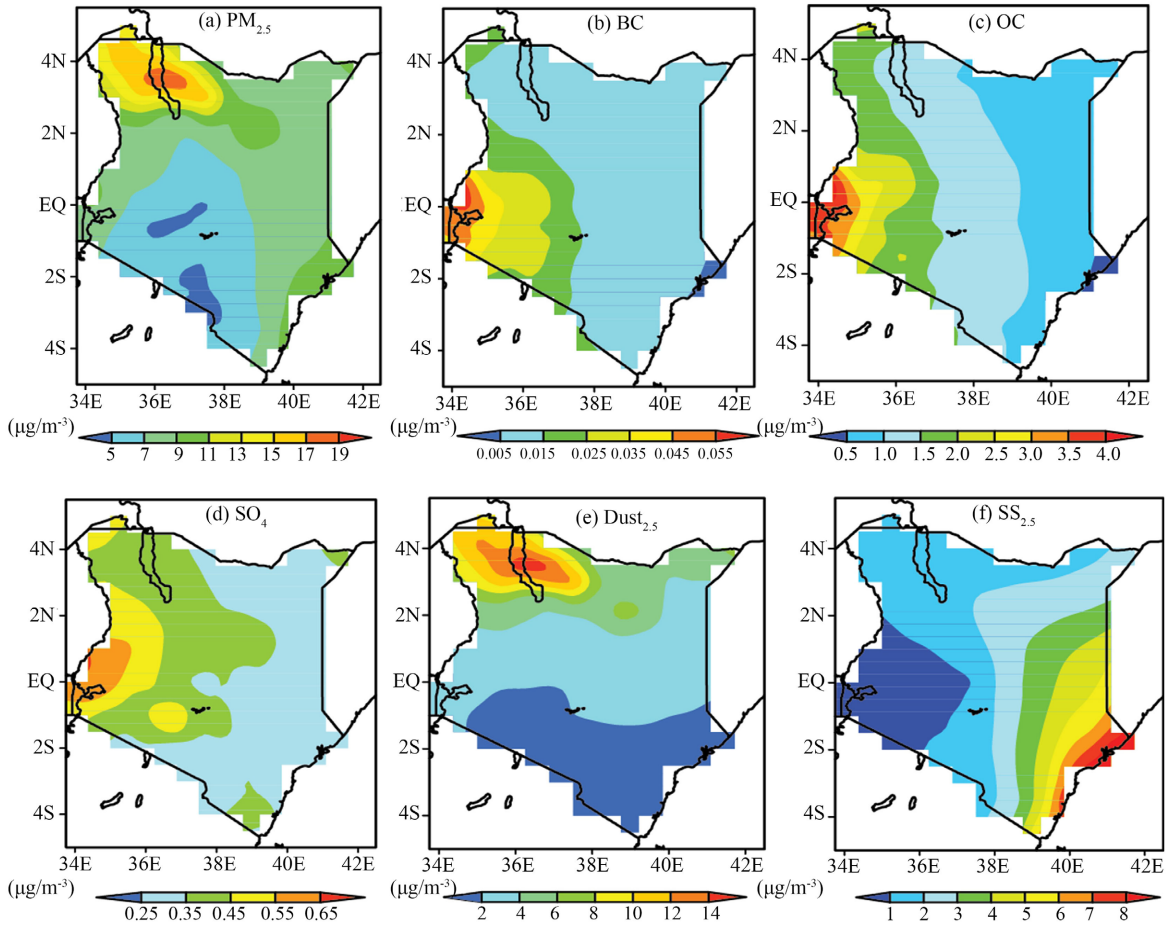

Figure 1. Spatial distribution of annual mean MERRA-2 $PM_{2.5}$ and its components, including (b) Black Carbon (BC), (c) Organic Carbon (OC), (d) Sulphate (SO_4), (e) Dust, (f) Sea Salt (SS) over Kenya during 1980-2020.

Sea salt $PM_{2.5}$ constituted 29.46% of $PM_{2.5}$ concentration. It is highly concentrated in the Coastal region **Figure 1(f)** because of the presence of the Indian Ocean. Sea salt $PM_{2.5}$ concentration records a high value of >8 $\mu g \cdot m^{-3}$. The concentration decreases as the distance from the Coast (Southeast) increases towards the West of the country. Organic carbon and black carbon accounted for 15.93% and 1.73% of $PM_{2.5}$ concentration, respectively. Their values were found high in the western region around the Lake Victoria **Figure 1(b)** and **Figure 1(c)**. It is a highly vegetated area and there is Lake Victoria therefore, activities such as fishing are carried out. This leads to anthropogenic activities like biomass burning which may be the main cause of high BC and OC concentrations. On the other hand, SO_4 contributes to 4.54% of $PM_{2.5}$ concentration, being high (>0.55 $\mu g \cdot m^{-3}$) over the Western part of the study domain. This could be caused by emissions from industries. It is observed that BC had the lowest percentage contribution to $PM_{2.5}$ with its values recording <1 $\mu g \cdot m^{-3}$ in regions where it is concentrated. Whereas $dust_{2.5}$ had the largest portion of $PM_{2.5}$ and recorded high values (>12 $\mu g \cdot m^{-3}$) over the Northern region. Thus $PM_{2.5}$ in Kenya is majorly constituted by dust which is naturally produced over the arid and semi-arid parts of the North Kenya.

3.1.2. Seasonal Distributions

The monthly datasets of $PM_{2.5}$ and its components (BC, OC, SO_4, $Dust_{2.5}$, $SS_{2.5}$) were averaged to make climatology for each season *i.e.*, local wet (MAM, OND) and local dry (JF, JJAS) seasons during each year over the study domain. The seasonal mean values obtained for each year were also averaged with the corresponding seasons during the study period (1980-2020) to make long-term climatological values of $PM_{2.5}$ and its components, for individual seasons.

The seasonal patterns of $PM_{2.5}$ and its components over Kenya derived from MERRA-2 shown in **Figure 2** are consistent with respective annual patterns **Figure 1**. The seasonal variations of $PM_{2.5}$ over Kenya are highly related to the seasonality of climatic conditions and anthropogenic activities [28]. High $PM_{2.5}$ concentration (>12 $\mu g \cdot m^{-3}$) over Kenya's atmosphere was observed during the local dry seasons (JF followed by JJAS and OND) noticed over the dust-dominant zones of Northwest Kenya. On the other hand, very low $PM_{2.5}$ values (<6 $\mu g \cdot m^{-3}$) were found during the local wet season (MAM months) characterized by high precipitation over the West and Central areas of Kenya. The reduced $PM_{2.5}$ concentration during MAM could be associated with enhanced precipitation that suppresses the emission of dust and washout of $PM_{2.5}$ in the atmosphere, in addition to reduced anthropogenic activities such as biomass burning. Hence, it is evident that the seasonal patterns of $PM_{2.5}$ are closely associated with the seasonal cycle of precipitation [36] depicting an inverse relationship between them.

On the other hand, the enhanced $PM_{2.5}$ loading during local dry seasons (JF and JJAS) could be attributed to an increased amount of anthropogenic activities such as land preparations, biomass burning, combustion of fossil fuels, vehicular and industrial emissions, and forest fires which release a significant amount of smoke particles into the atmosphere [28] [37]. Furthermore, the dry seasons are

characterized by intense solar radiation which leads to terrain heating. The stronger near-surface winds during JJAS over the arid and semi-arid areas of the Northwest parts of Kenya could accelerate the formation of dust particles. Thus, high temperatures in association with strong winds, create a strong convection that results in the upward movement of loose soil contribute to increased SS and hence high PM values during the local dry seasons [34] [35]. In terms of area coverage and strength of PM components, seasonal spatial distribution is related to annual distribution. Each component concentration was found high during JF followed by JJAS and OND months, and minimum during MAM.

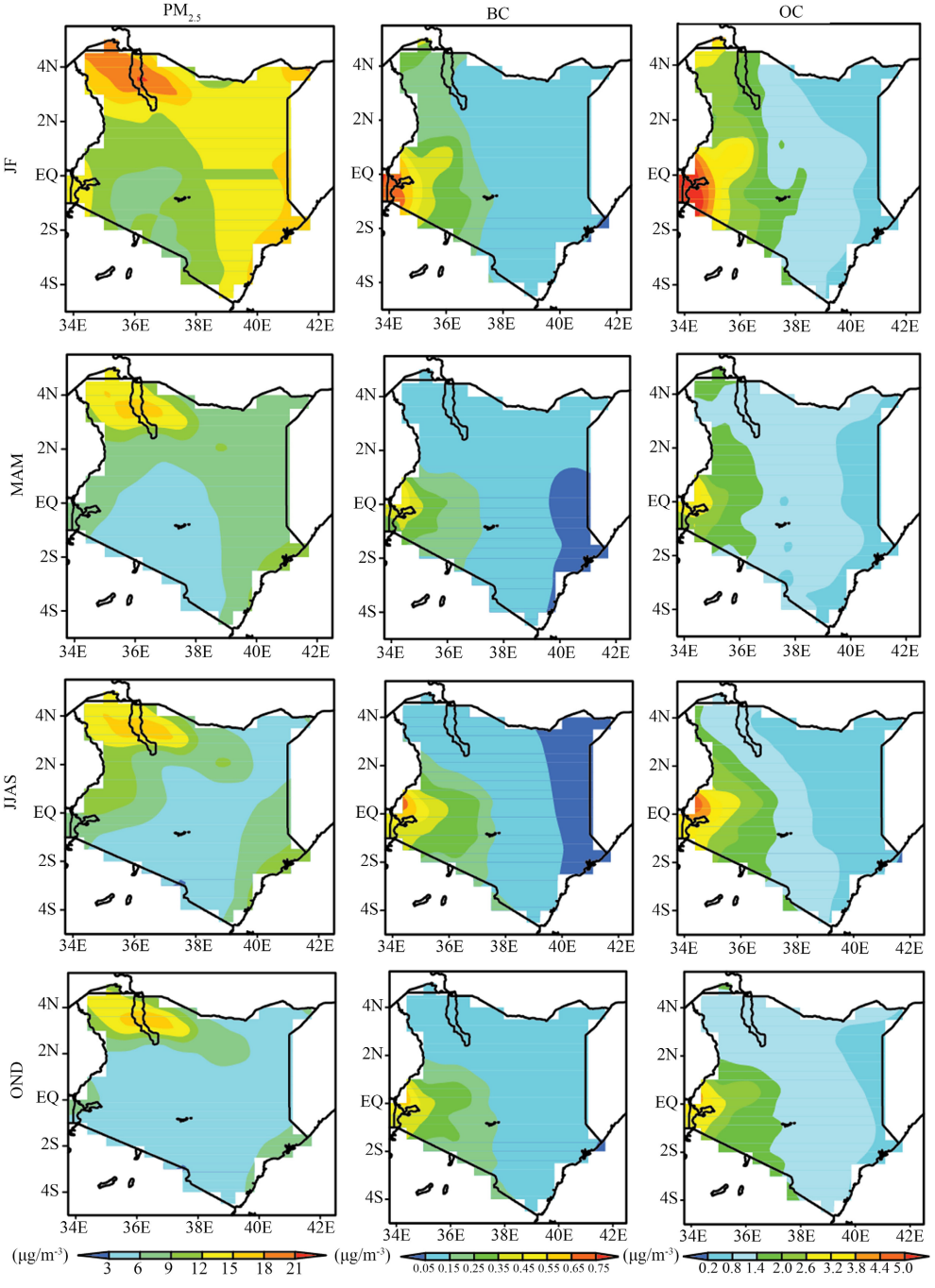

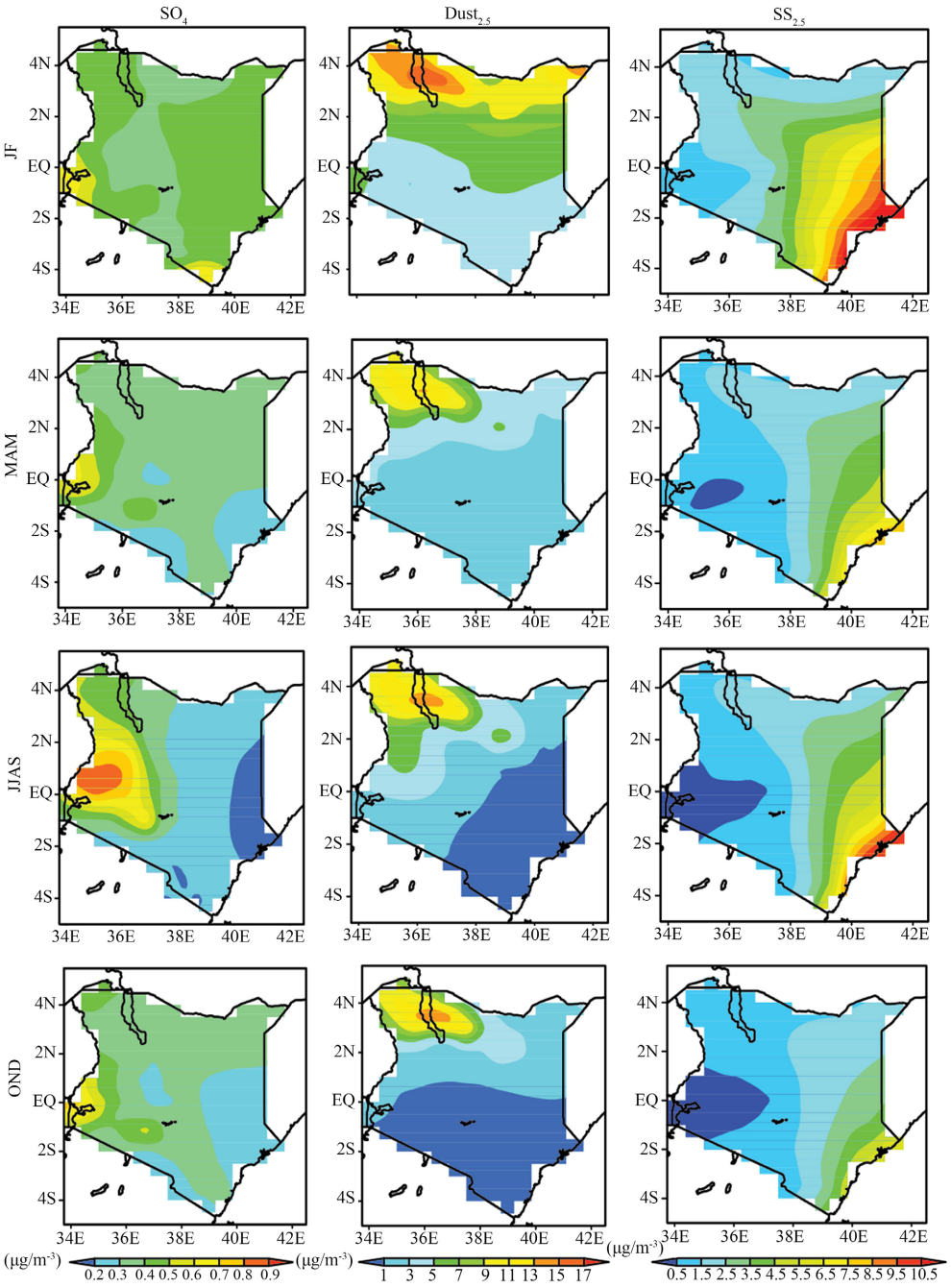

Figure 2. Seasonal variation of MERRA-2 $PM_{2.5}$ and its components over Kenya during 1980-2020.

3.2. Spatiotemporal Trends in MERRA-2 $PM_{2.5}$ and Its Components

3.2.1. Linear Trends

The inter-annual mean changes of MERRA-2 $PM_{2.5}$ and these individual components over Kenya during 1980-2020 is shown in **Figure 3**. Overall, $PM_{2.5}$ and its components (BC, OC SO_4, Dust and SS) fluctuate from year to year and decade to decade as observed by MERRA-2. There was a gradual increasing trend in $PM_{2.5}$ up to 2011 where it was at its highest peak reached to 12.6 $\mu g \cdot m^{-3}$. After 2011 there is a transition from increasing to decreasing concentrations for the

rest of the period. Similarly, the results showed a similar growth trend for SO_4 and a significant turning point from increasing to decreasing in 2011. Comparable trends were also found in BC and OC, but their values exhibited much higher in 2020. In addition, dust and SS showed a progressive increase after 1980. Notably, the increasing trend in $PM_{2.5}$ components has been increasing over the years after 1980. Generally, the inter-annual variability in $PM_{2.5}$ and its individual components over Kenya is influenced by changes in anthropogenic emissions and meteorology. The major PM emissions are dust emissions over the arid and semi-arid areas in the North Kenya depicted with low annual rainfall [28]. Other $PM_{2.5}$ emissions are considered as the anthropogenic emissions resulting from industrial-vehicular emissions, forest burning, and agricultural and biomass burning [20] [21] [24] attributed to increased concentrations.

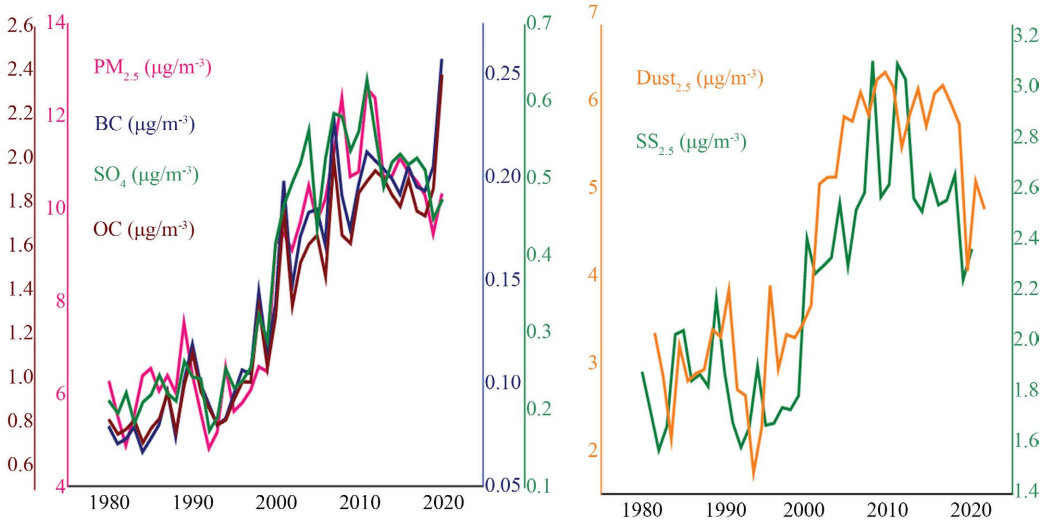

Figure 3. The annual mean trends in MERRA-2 $PM_{2.5}$ and its five major components over Kenya from 1980 to 2020.

3.2.2. Spatial Trends

The spatial distribution of annual $PM_{2.5}$ and its components (BC, OC, SO_4, Dust and SS) trends retrieved from MERRA-2 is shown in **Figure 4**. The observed positive trend implies an increase in $PM_{2.5}$ concentration, whereas the negative trends interpret a reduced levels of $PM_{2.5}$. Comparing the patterns of variation observed in the spatial trends with the averaged annual and seasonal distribution **Figure 1**, and **Figure 2**), it is revealed that positive trends generally correspond to high $PM_{2.5}$ regions and vice-versa. This signifies the role of emission sources in enhancing $PM_{2.5}$ concentrations over Kenya. An overall increase in annual $PM_{2.5}$ trends was observed with a significant trend of 95% over most regions in Kenya. The trends were significant over the arid and semi-arid areas of the Northern and Eastern parts of Kenya **Figure 4(a)** dominated by dust. The increased trend could be associated with reduced precipitation and wind speed resulting in an increase in locally generated dust [35] [38]. Negative trends for Dust, SO_4 and SS were observed in the Western and Central regions of Kenya at-

tributed to dense coverage by vegetation and high altitudes relative to rest of the domain. These regions also experience increased precipitation and, therefore, no exposure of soil to an increased concentration of $PM_{2.5}$ and its individual components. Dust is the major component contributing to high $PM_{2.5}$. An increasing trend of dust is observed over the Northwest part of Kenya **Figure 4(e)**. This is due to increased temperature loosening the soil and eventually exposure to the atmosphere [28]. For OC and BC, an increasing trend is observed over the Western region of Kenya **Figure 4(b)** and **Figure 4(c)**. The increasing trend is caused by anthropogenic activities such as biomass burning, combustion of fossil fuels, vehicular and industrial emissions [34]. **Figure 4(d)** reveals an increasing trend of SO_4 over the North and Eastern areas of Kenya. This is attributed to rapid industrialization and urbanization within those areas. Sea salt is mainly originated from the Indian Ocean and therefore, increasing in sea salt is observed on the Coast.

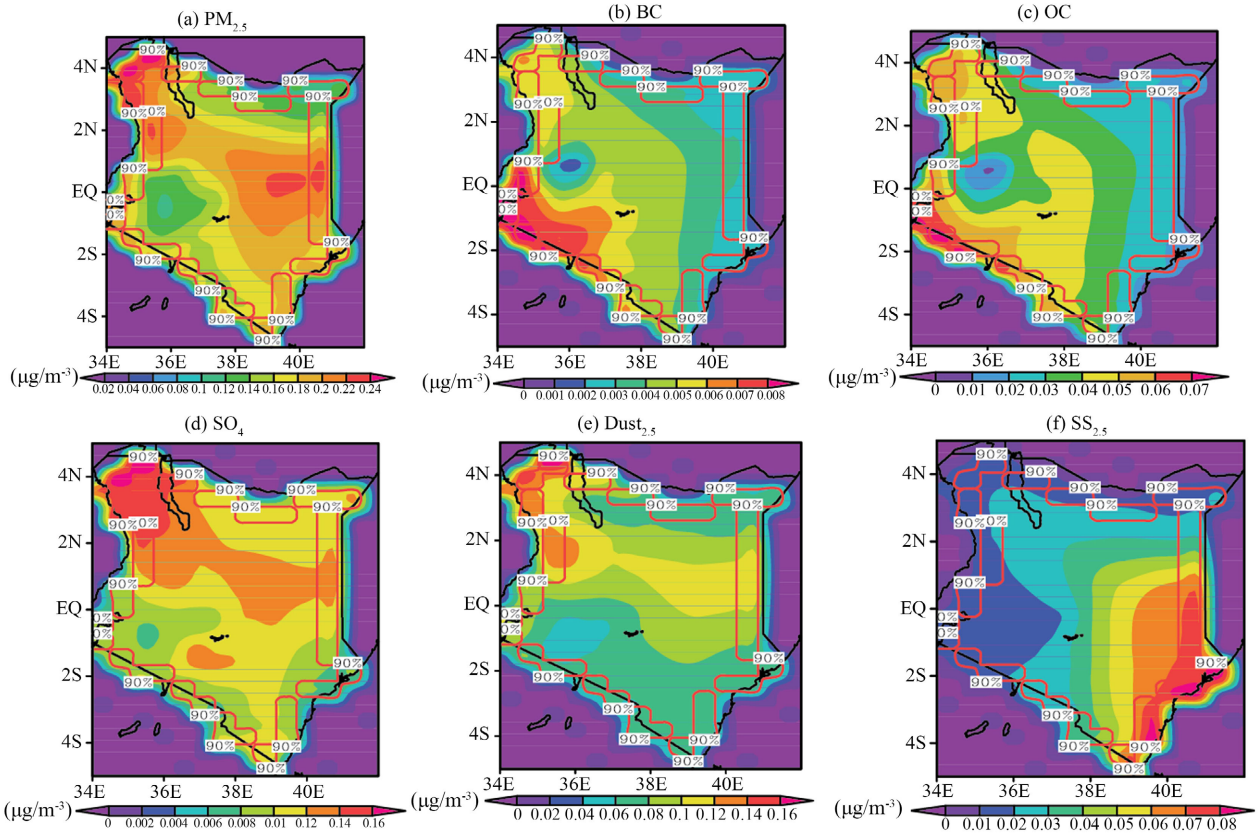

Figure 4. The annual trends of MERRA-2 $PM_{2.5}$ and its individual components, including (a) the $PM_{2.5}$ (b) Black Carbon $PM_{2.5}$ (c) Organic Carbon $PM_{2.5}$ (d) Sulphate $PM_{2.5}$ (e) Dust $PM_{2.5}$ (f) Sea Salt $PM_{2.5}$ over Kenya during 1980-2020.

3.3. Spatial Correlations between MERRA-$PM_{2.5}$ and Its Components

The spatial correlations of PM and its components (BC, OC, SO_4, Dust and SS) derived from MERRA-2 over Kenya during the study period are shown in **Figure 5**. The spatial correlation revealed areas of similarities/dissimilarities and the

magnitude of the correlation coefficient (r). A high correlation coefficient (>0.8) was observed in the PM-Dust correlation **Figure 5(d)** over most areas in the study domain. It is also observed in the PM-SO_4 correlation over the Southeast of Kenya. A moderate to high correlation coefficient (>0.5 - 0.8) was observed in PM-SO_4 **Figure 5(c)** and PM-SS **Figure 5(e)** correlation over the East and South of Kenya, respectively. On the other hand, a low correlation coefficient was observed in PM-BC **Figure 5(a)** and PM-OC **Figure 5(b)** over most areas in the study domain. The study reveals that PM distribution is largely contributed by dust. Dust is dominated in arid and semi-arid areas in the Northern region of the study domain. The region experiences high temperatures which intensify surface heating loosening the soil and resulting in an increased convection hence higher $PM_{2.5}$ loading.

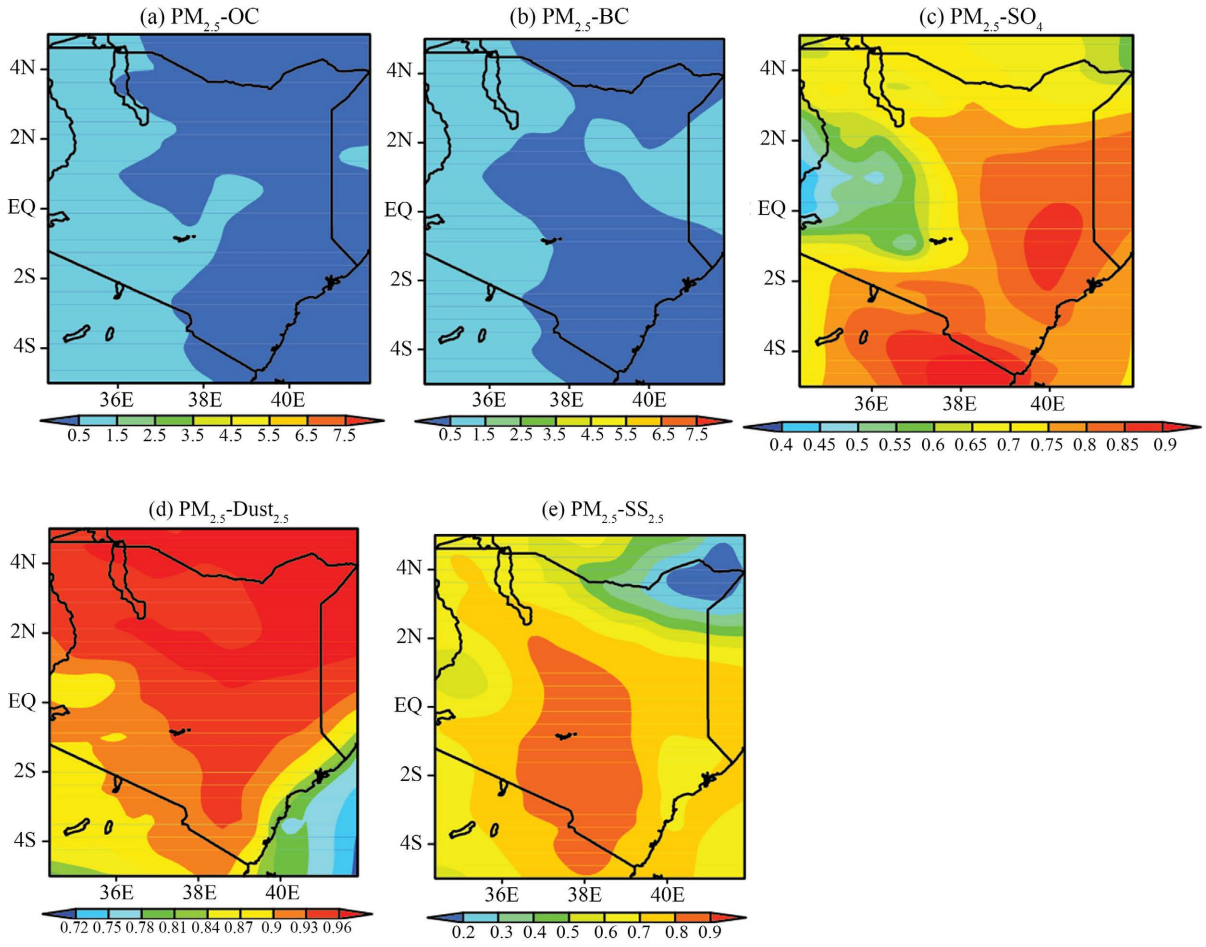

Figure 5. Spatial correlations of MERRA $PM_{2.5}$ and its components including (a) $PM_{2.5}$-OC, (b) $PM_{2.5}$-BC, (c) $PM_{2.5}$-SO_4, (d) $PM_{2.5}$-$Dust_{2.5}$, (e) $PM_{2.5}$-$SS_{2.5}$ over Kenya during 1980 to 2020.

4. Summary and Conclusions

Using 41 years (1980-2020) annual/seasonal data retrieved from MERRA-2, this study presented an in-depth understanding of spatial-temporal distribution in $PM_{2.5}$ and components (BC, OC, SO_4, Dust and SS) over Kenya as well as ex-

amined the correlation between PM and its components. The spatial patterns of annual mean $PM_{2.5}$ over Kenya were generally characterized by low (<7 $\mu g \cdot m^{-3}$), moderate (7 - 9 $\mu g \cdot m^{-3}$) and high (>11 $\mu g \cdot m^{-3}$) concentrations. Low $PM_{2.5}$ concentrations were observed in high altitude and densely vegetated regions in Western and Central parts of Kenya. Moderate $PM_{2.5}$ concentrations were observed in the Western, Eastern and North Rift parts of Kenya attributed to anthropogenic activities. These places experience moderate temperatures. Peak distribution of $PM_{2.5}$ concentrations was observed over dust-dominant arid and semi-arid areas of North West regions of Kenya. $PM_{2.5}$ components BC and OC concentration were dominant in the Western region of Kenya due to anthropogenic activities in that region. SO_4 concentration was also high in most parts of the country, a carbonaceous emission from industries. On the other hand, SS concentration was high in the South East region of Kenya due to the fact its emission is majorly from the Indian Ocean. Whereas, dust concentration was relatively high in dust-dominated arid and semi-arid regions of the Northern part of Kenya. Dust exhibited the highest percentage contribution to $PM_{2.5}$ concentrations. The seasonal $PM_{2.5}$ climatology over the entire study domain was consistent with that of annual patterns, being low during the local wet seasons and high during local dry seasons. This was attributed to seasonality in emission sources, anthropogenic activities and meteorological factors such as temperature, wind speed, precipitation and relative humidity.

Analysis of $PM_{2.5}$ and components trends over Kenya during 1980-2020 showed a significant increase over the years. Positive trends were observed over dust-dominated areas that are over the Northern region of Kenya and sparingly for SO_4. BC and OC showed positive trends around Lake Victoria in the Western region of Kenya. On the other hand, SS was relatively positive in the Coastal region of Kenya.

This work conclusively compared the spatial correlation of $PM_{2.5}$ and its components. $PM_{2.5}$-Dust correlation exhibited a strong correlation in most parts of the study domain, showing the significant contribution of the components to $PM_{2.5}$ over the study domain. It had the highest correlation coefficient, followed by SO_4. A low correlation coefficient was observed between $PM_{2.5}$ and OC. Notably, change in emissions has a potential effect of adversely affecting $PM_{2.5}$ trends over Kenya. In order to investigate this in detail, revealing the casual relationship, a modelling study is planned as a future research project.

Conflicts of Interest

The authors declare no conflicts of interest.

References

[1] World Health Organization (WHO) (2006) Air Quality Guidelines for Particulate Matter, Ozone, Nitrogen Dioxide and Sulfur Dioxide-Global Update 2005-Summary of Risk Assessment. Geneva.
https://www.who.int/publications/i/item/WHO-SDE-PHE-OEH-06-02

[2] Environmental Protection Agency (EPA) (2016) Particulate Matter Pollution. https://www.epa.gov/pm-pollution/particulate-matter-pm-basics

[3] Jaiprakash, Singhai, A., Habib, G., Raman, R.S. and Gupta, T. (2016) Chemical Characterization of $PM_{1.0}$ Aerosol in Delhi and Source Apportionment Using Positive Matrix Factorization. *Environmental Science and Pollution Research*, **24**, 445-462. https://doi.org/10.1007/s11356-016-7708-8

[4] Liu, L., Breitner, S., Schneider, A., Cyrys, J., Brüske, I., Franck, U., *et al.* (2013) Size-Fractioned Particulate Air Pollution and Cardiovascular Emergency Room Visits in Beijing, China. *Environmental Research*, **121**, 52-63. https://doi.org/10.1016/j.envres.2012.10.009

[5] Meng, X., Ma, Y., Chen, R., Zhou, Z., Chen, B. and Kan, H. (2013) Size-Fractionated Particle Number Concentrations and Daily Mortality in a Chinese City. *Environmental Health Perspectives*, **121**, 1174-1178. https://doi.org/10.1289/ehp.1206398

[6] Mukherjee, A. and Agrawal, M. (2017) A Global Perspective of Fine Particulate Matter Pollution and Its Health Effects. In: de Voogt, P., Ed., *Reviews of Environmental Contamination and Toxicology*, Springer International Publishing, 5-51. https://doi.org/10.1007/398_2017_3

[7] Kinney, P.L., Gichuru, M.G., Volavka-Close, N., Ngo, N., Ndiba, P.K., Law, A., *et al.* (2011) Traffic Impacts on $PM_{2.5}$ Air Quality in Nairobi, Kenya. *Environmental Science & Policy*, **14**, 369-378. https://doi.org/10.1016/j.envsci.2011.02.005

[8] Thurston, G.D., Ahn, J., Cromar, K.R., Shao, Y., Reynolds, H.R., Jerrett, M., *et al.* (2016) Ambient Particulate Matter Air Pollution Exposure and Mortality in the NIH-AARP Diet and Health Cohort. *Environmental Health Perspectives*, **124**, 484-490. https://doi.org/10.1289/ehp.1509676

[9] World Health Orgaization (WHO) (2012) Exposure to Particulate Matter with an Aerodynamic Diameter of 10 Micrometer or Less (PM_{10}) in 1100 Urban Areas, 2003-2012.

[10] Egondi, T., Ettarh, R., Kyobutungi, C., Ng, N. and Rocklöv, J. (2018) Exposure to Outdoor Particles ($PM_{2.5}$) and Associated Child Morbidity and Mortality in Socially Deprived Neighborhoods of Nairobi, Kenya. *Atmosphere*, **9**, Article No. 351. https://doi.org/10.3390/atmos9090351

[11] Kaufman, Y.J., Tanré, D. and Boucher, O. (2002) A Satellite View of Aerosols in the Climate System. *Nature*, **419**, 215-223. https://doi.org/10.1038/nature01091

[12] Stocker, T., Plattner, G., Tignor, M., Qin, D., Allen, S., Boschung, J., Nauels, A., Xia, Y., Bex, V. and Midgley, P. (2013) The Physical Science Basis: Summary for Policy Makers. Climate Change. https://www.ipcc.ch/report/ar5/wg1/

[13] Gupta, P., Christopher, S.A., Wang, J., Gehrig, R., Lee, Y. and Kumar, N. (2006) Satellite Remote Sensing of Particulate Matter and Air Quality Assessment over Global Cities. *Atmospheric Environment*, **40**, 5880-5892. https://doi.org/10.1016/j.atmosenv.2006.03.016

[14] Wang, S., Zhou, C., Wang, Z., Feng, K. and Hubacek, K. (2017) The Characteristics and Drivers of Fine Particulate Matter ($PM_{2.5}$) Distribution in China. *Journal of Cleaner Production*, **142**, 1800-1809. https://doi.org/10.1016/j.jclepro.2016.11.104

[15] He, L., Lin, A., Chen, X., Zhou, H., Zhou, Z. and He, P. (2019) Assessment of MERRA-2 Surface $PM_{2.5}$ over the Yangtze River Basin: Ground-Based Verification, Spatiotemporal Distribution and Meteorological Dependence. *Remote Sensing*, **11**, Article No. 460. https://doi.org/10.3390/rs11040460

[16] Petkova, E.P., Jack, D.W., Volavka-Close, N.H. and Kinney, P.L. (2013) Particulate Matter Pollution in African Cities. *Air Quality, Atmosphere & Health*, **6**, 603-614.

https://doi.org/10.1007/s11869-013-0199-6

[17] Onyango, S., Parks, B., Anguma, S. and Meng, Q. (2019) Spatio-Temporal Variation in the Concentration of Inhalable Particulate Matter (PM_{10}) in Uganda. *International Journal of Environmental Research and Public Health*, **16**, Article No. 1752. https://doi.org/10.3390/ijerph16101752

[18] Singh, A., Ng'ang'a, D., Gatari, M.J., Kidane, A.W., Alemu, Z.A., Derrick, N., *et al.* (2021) Air Quality Assessment in Three East African Cities Using Calibrated Low-Cost Sensors with a Focus on Road-Based Hotspots. *Environmental Research Communications*, **3**, Article ID: 075007. https://doi.org/10.1088/2515-7620/ac0e0a

[19] Tesema, G.A., Teshale, A.B. and Tessema, Z.T. (2021) Incidence and Predictors of Under-Five Mortality in East Africa Using Multilevel Weibull Regression Modeling. *Archives of Public Health*, **79**, Article No. 196. https://doi.org/10.1186/s13690-021-00727-9

[20] van Vliet, E.D.S. and Kinney, P.L. (2007) Impacts of Roadway Emissions on Urban Particulate Matter Concentrations in Sub-Saharan Africa: New Evidence from Nairobi, Kenya. *Environmental Research Letters*, **2**, Article ID: 045028. https://doi.org/10.1088/1748-9326/2/4/045028

[21] Ngo, N.S., Gatari, M., Yan, B., Chillrud, S.N., Bouhamam, K. and Kinney, P.L. (2015) Occupational Exposure to Roadway Emissions and Inside Informal Settlements in Sub-Saharan Africa: A Pilot Study in Nairobi, Kenya. *Atmospheric Environment*, **111**, 179-184. https://doi.org/10.1016/j.atmosenv.2015.04.008

[22] Egondi, T., Muindi, K., Kyobutungi, C., Gatari, M. and Rocklöv, J. (2016) Measuring Exposure Levels of Inhalable Airborne Particles ($PM_{2.5}$) in Two Socially Deprived Areas of Nairobi, Kenya. *Environmental Research*, **148**, 500-506. https://doi.org/10.1016/j.envres.2016.03.018

[23] Kenya National Bureau of Statistics (KNBS) (2019) Ministry of Planning. Republic of Kenya Economic Survey 2019.

[24] Makokha, J.W. and Angeyo, H.K. (2013) Investigation of Radiative Characteristics of the Kenyan Atmosphere Due to Aerosols Using Sun Spectrophotometry Measurements and the COART Model. *Aerosol and Air Quality Research*, **13**, 201-208. https://doi.org/10.4209/aaqr.2012.06.0146

[25] Ongoma, V. and Chen, H. (2017) Temporal and Spatial Variability of Temperature and Precipitation over East Africa from 1951 to 2010. *Meteorology and Atmospheric Physics*, **129**, 131-144.

[26] Ayugi, B., Tan, G., Ullah, W., Boiyo, R. and Ongoma, V. (2019) Inter-Comparison of Remotely Sensed Precipitation Datasets over Kenya during 1998-2016. *Atmospheric Research*, **225**, 96-109. https://doi.org/10.1016/j.atmosres.2019.03.032

[27] Yang, W., Seager, R., Cane, M.A. and Lyon, B. (2015) The Annual Cycle of East African Precipitation. *Journal of Climate*, **28**, 2385-2404. https://doi.org/10.1175/jcli-d-14-00484.1

[28] Boiyo, R., Kumar, K.R. and Zhao, T. (2018) Spatial Variations and Trends in AOD Climatology over East Africa during 2002-2016: A Comparative Study Using Three Satellite Data Sets. *International Journal of Climatology*, **38**, e1221-e1240. https://doi.org/10.1002/joc.5446

[29] Buchard, V., da Silva, A.M., Randles, C.A., Colarco, P., Ferrare, R., Hair, J., *et al.* (2016) Evaluation of the Surface $PM_{2.5}$ in Version 1 of the NASA MERRA Aerosol Reanalysis over the United States. *Atmospheric Environment*, **125**, 100-111. https://doi.org/10.1016/j.atmosenv.2015.11.004

[30] Zhang, J. and Reid, J.S. (2010) A Decadal Regional and Global Trend Analysis of the

Aerosol Optical Depth Using a Data-Assimilation Grade Over-Water MODIS and Level 2 MISR Aerosol Products. *Atmospheric Chemistry and Physics*, **10**, 10949-10963. https://doi.org/10.5194/acp-10-10949-2010

[31] Kumar, K.R., Sivakumar, V., Yin, Y., Reddy, R.R., Kang, N., Diao, Y., *et al.* (2014) Long-Term (2003-2013) Climatological Trends and Variations in Aerosol Optical Parameters Retrieved from MODIS over Three Stations in South Africa. *Atmospheric Environment*, **95**, 400-408. https://doi.org/10.1016/j.atmosenv.2014.07.001

[32] Kumar, K.R., Yin, Y., Sivakumar, V., Kang, N., Yu, X., Diao, Y., *et al.* (2015) Aerosol Climatology and Discrimination of Aerosol Types Retrieved from MODIS, MISR and OMI over Durban (29.88˚S, 31.02˚E), South Africa. *Atmospheric Environment*, **117**, 9-18. https://doi.org/10.1016/j.atmosenv.2015.06.058

[33] Hu, K., Kumar, K.R., Kang, N., Boiyo, R. and Wu, J. (2017) Spatiotemporal Characteristics of Aerosols and Their Trends over Mainland China with the Recent Collection 6 MODIS and OMI Satellite Datasets. *Environmental Science and Pollution Research*, **25**, 6909-6927. https://doi.org/10.1007/s11356-017-0715-6

[34] Boiyo, R., Kumar, K.R., Zhao, T. and Bao, Y. (2017) Climatological Analysis of Aerosol Optical Properties over East Africa Observed from Space-Borne Sensors during 2001-2015. *Atmospheric Environment*, **152**, 298-313. https://doi.org/10.1016/j.atmosenv.2016.12.050

[35] Ngaina, J., Mutai, B., Ininda, J. and Muthama, J. (2014) Monitoring Spatial-Temporal Variability of Aerosol over Kenya. *Ethiopian Journal of Environmental Studies and Management*, **7**, 244-252. https://doi.org/10.4314/ejesm.v7i3.3

[36] de Graaf, M., Tilstra, L.G., Aben, I. and Stammes, P. (2010) Satellite Observations of the Seasonal Cycles of Absorbing Aerosols in Africa Related to the Monsoon Rainfall, 1995-2008. *Atmospheric Environment*, **44**, 1274-1283. https://doi.org/10.1016/j.atmosenv.2009.12.038

[37] Makokha, J.W., Odhiambo, J.O. and Godfrey, J.S. (2017) Trend Analysis of Aerosol Optical Depth and Ångström Exponent Anomaly over East Africa. *Atmospheric and Climate Sciences*, **7**, 588-603. https://doi.org/10.4236/acs.2017.74043

[38] Gatebe, C.K., Tyson, P.D., Annegarn, H.J., Helas, G., Kinyua, A.M. and Piketh, S.J. (2001) Characterization and Transport of Aerosols over Equatorial Eastern Africa. *Global Biogeochemical Cycles*, **15**, 663-672. https://doi.org/10.1029/2000gb001340